Long-time Bell states of waveguide-mediated qubits via continuous measurement

Huiping Zhan and Huatang Tan[*]

Department of Physics, Huazhong Normal University, Wuhan 430079, China

In this paper we consider a scheme for achieving long-time sustainable Bell states of two distant qubits mediated by a one-dimensional waveguide whose outputs are subjected to time-continuous photon counting or homodyne detection. In both of the detection cases, it is shown that different Bell states can be obtained, for different initial states, in the long-time regime. In particular, we find that, in the case of photon counting, a cyclic jump among Bell states can be formed once the first photon is registered. While in the homodyne-detection case we further reveal that any steady Bell state can be achieved independent of detection efficiency, with a probability of 50% . The underlying physical reason for this is also analyzed. Our scheme is advantageous over previous studies in which only transient or intermittent Bell states can be generated. The long-time Bell states of distant qubits can be used for constructing quantum networks.

I. INTRODUCTION

Apart from fundamental interests of research, entanglement has nowadays become a core resource of quantum informatics [1]. Bell states, as maximally entangled two-qubit states, have perfect quantum correlations and are therefore especially important for realizing various high-efficient quantum tasks, such as quantum teleportation [2]. Many kinds of protocols were designed to generate Bell states in different quantum matters, like atomic systems, quantum dots, superconducting qubits, and the magnon-photon system [3–6]. Compared to such short-distance entanglement, long-distance entanglement is of importance for distributing and transmitting quantum information among distant quantum nodes in quantum networks [7,8]. To this end, new light was recently shed on waveguide QED systems, which are excellent integration platforms for generating long-distance entanglement and building waveguide quantum networks, owing to their characteristics of controllable interactions between matters and light and combining them with open propagation directions [9–22].

The studies for generating entanglement between two distant quantum emitters (qubits) mediated by, e.g., photonic, plasmonic, and magnonic waveguides have been carried out [23–27]. However, the only results are mixed entangled states due to the unavoidable decoherence process, such as spontaneous emission. As we know, the spontaneous emission process can be envisaged as an ensemble of trajectories of time-continuous quantum weak measurements on the environment induced by the decoherence process [28–32], pure Bell states of some trajectory may be generated via measurements, e.g., continuous photon counting and homodyne detection [33–37]. For example, it has recently been shown that short-time Bell states of quantum trajectories can be achieved by continuously homodyning the outputs of a beam splitter on

which the spontaneous fluorescences from two qubits are incident [36]. It was also shown that entangled states of two remote qubits connected with fiber can be achieved via homodyne detection [37]. The measurement provides information on the total spin of the two qubits such that the entanglement can be postselected. Experimentally, the entanglement of quantum trajectories of homodyne detection on two distant qubits has been demonstrated [38]. Nevertheless, the entangled states just appear in the transient regime and moreover the Bell states merely exist at some time points since the qubits initially prepared in excited states inevitably relax to ground states. To pull the qubits back to the excited states, one can employ a classical strong driving field. For instance, Zhang *et al.* [39] recently proposed a scheme for the heralded generation of the Bell state of waveguide-mediated qubits driven by a classical laser via continuous photon counting. However, the Bell state is merely present in an intermittent manner since it takes time for the qubits to revert back to excited states, and moreover the conditional Bell state almost collapses even when the detection efficiency deviates from the unit slightly.

In this paper, we consider a scheme for achieving long-term sustainable Bell states of two distant waveguide-mediated qubits via photon counting or homodyne detection. The system under our consideration consists of two laser-driven identical emitters in the Λ configuration which are coupled to a one-dimensional waveguide via off-resonant Raman scattering. The outputs of the waveguide are subject to continuous photon counting or homodyne detection. In both of these cases, it is shown that different types of Bell states can be realized in the long-time regime. For the photon-counting case, we find that a cyclic jump among Bell states is formed once the first photon is detected, meaning that different Bell states appear alternately, conditioned on the occurrence of subsequent photon-detection events. While for the homodyne detection case, we show that initial-state-dependent Bell states can be obtained in the regime of steady states, with a
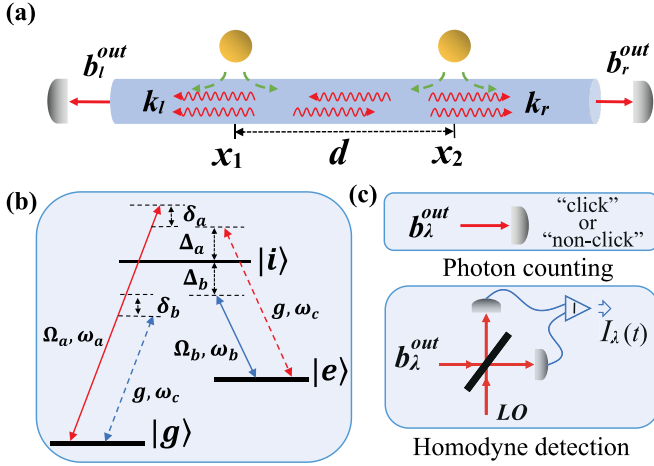
*tht@mail.ccnu.edu.cn

033715-1

FIG. 1. (a) A schematic plot of the system. Two identical Λ-type emitters are located at the positions $x_{1,2}$ along the waveguide and coupled to the left and right propagating waveguide modes $b_{l,r}$ with wave numbers $k_{l,r}$. The output fields $b_{l,r}^{out}$ of the waveguide are subject to photon counting or homodyne detection, as shown in (c). (b) Energy level diagram of the Λ-type emitters, in which the ground state $|g\rangle$ and excited state $|e\rangle$ are coupled to the auxiliary state $|i\rangle$ through the driving fields of frequency $\omega_{a,b}$ and the waveguide modes of frequency ω.

probability of 50%. Moreover, this is independent of homodyne detection efficiency.

The remainder of the paper is organized as follows. In Secs. II and III, the system and the working equations are presented. In Sec. VI, we investigate in detail the properties of the entanglement of trajectories via photon counting and homodyne detection. In the last section, the summary is given.

II. SYSTEM AND EQUATIONS

As schematically shown in Fig. 1(a), our system consists of two identical emitters in the Λ configuration coupled to a one-dimensional waveguide with distance d. Each emitter is driven by classical fields with frequencies ω_i ($i = a, b$) and simultaneously coupled to the left and right transmitting waveguide modes $\hat{b}_\lambda$ ($\lambda = l, r$) with frequency ω and wave vector k_λ, as depicted in Fig. 1(b). The total Hamiltonian of our system is given by [40]

$$\hat{H}_{\text{sys}} = \hat{H}_0 + \hat{H}_I, \tag{1}$$

with

$$\hat{H}_0 = \sum_{j=1,2} (\omega_g \hat{\sigma}_{gg} + \omega_w \hat{\sigma}_{ee} + \hat{\omega}_i \sigma_{ii})$$

$$+ \sum_{\lambda=l,r} \int \omega \hat{b}_\lambda(\omega)^\dagger \hat{b}_\lambda(\omega) d\omega, \tag{2}$$

$$\hat{H}_I = i \sum_{\lambda=l,r} \sum_{j=1,2} \int \left[(g\hat{b}_\lambda(\omega) e^{ik_\lambda x_j} + \Omega_a e^{-i\omega_a t}) \hat{\sigma}_{ig}^j \right.$$

$$\left. + (g\hat{b}_\lambda(\omega) e^{ik_\lambda x_j} + \Omega_b e^{-i\omega_b t}) \hat{\sigma}_{ie}^j \right] d\omega + \text{H.c.}, \tag{3}$$

where g and Ω_i are the coupling strengths of atom-waveguide and atom-field. x_j denotes the position of atom j along the

waveguide. $\hat{\sigma}_{mn} = |m\rangle\langle n| (m, n = g, e, i)$ are the atomic transition operators, with the corresponding frequency ω_{mn}. In the interaction picture with respect to the free Hamiltonian $\hat{H}_0$, the effective Hamiltonian of the entire system can be written as

$$\hat{H}_{\text{eff}}(t) = i \sum_{\lambda=l,r} \sum_{j=1,2} \int \left[g\hat{b}_\lambda(\omega) \hat{\sigma}_{ig}^j e^{ik_\lambda x_j} e^{i(\Delta_b + \delta_b)t} \right.$$

$$+ g\hat{b}_\lambda(\omega) \hat{\sigma}_{ie}^j e^{ik_\lambda x_j} e^{-i\Delta_a t} + \Omega_a \hat{\sigma}_{ig}^j e^{-i(\Delta_a + \delta_a)t}$$

$$\left. + \Omega_b \hat{\sigma}_{ie}^j e^{i\Delta_b t} \right] d\omega + \text{H.c.}, \tag{4}$$

describing the coupling of the emitters at positions $x_{1,2}$ to the driving fields and the waveguide (as a reservoir). Here the detunings $\Delta_a = \omega - \omega_{ie}$, $\Delta_b = \omega_{ie} - \omega_b$, $\delta_a = \omega_a - \omega_{eg} - \omega$, and $\delta_b = \omega_b + \omega_{eg} - \omega$. Consider the situations: the detuning $|\Delta_i| \gg |\Omega_i|$, such that the excited state $|i\rangle$ can be adiabatically eliminated; the dispersive atom-waveguide interaction from the adiabatical elimination can be ignored for the condition $|\Omega_i| \gg |g|$. Then we follow the methods as in Ref. [41] and derive the effective Hamiltonian

$$\tilde{\tilde{H}}_{\text{eff}} = -i\hat{H}_{\text{eff}}(t) \int dt' \hat{H}_{\text{eff}}(t'), \tag{5}$$

thus $\tilde{\tilde{H}}_{\text{eff}} = \tilde{\tilde{H}}_0 + \tilde{H}_I$ is obtained, with

$$\tilde{\tilde{H}}_0 = \sum_{j=1,2} \frac{1}{2} \tilde{\omega} \hat{\sigma}_z^j, \tag{6a}$$

$$\tilde{H}_I = i \sqrt{\frac{\gamma}{2\pi}} \sum_{\lambda=l,r} \sum_{j=1,2} \int \hat{b}_\lambda^\dagger(\omega)(\hat{\sigma}_j + \hat{\sigma}_j^\dagger) e^{-i(k_\lambda x_j + \delta t)} d\omega$$

$$+ \text{H.c.}, \tag{6b}$$

on the conditions $\delta_a = -\delta_b = \delta$ and $|\Delta_a/\Delta_b| = |\Omega_a/\Omega_b|$. Here, $\tilde{\tilde{H}}_0$ is the free Hamiltonian of a two-level emitter with the transition frequency $\tilde{\omega} = -\sum_i \frac{4|\Omega_i|^2}{\Delta_i}$ between the energy levels $|e\rangle$ and $|g\rangle$ (as our qubit). $\tilde{H}_I$ describes effective interaction between the qubits and the waveguide, with $\gamma/2\pi = 4 | g\Omega_i/\Delta_i |^2$ and the lowering operator $\hat{\sigma}_j = \hat{\sigma}_{ge}^j (\hat{\sigma}_j^\dagger = \hat{\sigma}_{eg}^j)$. For the initial vacuum of the waveguide modes, the master equation for the density operator $\hat{\rho}_a$ of the qubits under the Born-Markovian approximation can be derived as [42,43]

$$\frac{d}{dt} \hat{\rho}_a = -i[\tilde{\tilde{H}}_0, \hat{\rho}_a] + \gamma \sum_{\lambda=l,r} \mathcal{D}[\hat{J}_{\lambda\pm}] \hat{\rho}_a, \tag{7}$$

with the distance $kd = 2n\pi$ or $(2n + 1)\pi$ for integer number n and $k_r = -k_l = k$. The symbol $\mathcal{D}[\hat{O}]\hat{\rho} = \hat{O}\hat{\rho}\hat{O}^\dagger - \{\hat{O}^\dagger \hat{O}, \hat{\rho}\}/2$, where the operators $\hat{J}_{\lambda\pm} = \hat{J}_1 \pm \hat{J}_2$, respectively, for $kd = 2n\pi$ and $kd = 2(n + 1)\pi$, with $\hat{J}_{j=1,2} = (\hat{\sigma}_j + \hat{\sigma}_j^\dagger)/\sqrt{2}$. Equation (7) effectively describes the dissipative-driven collective dynamics of two qubits immersed in a one-dimensional bosonic environment. Note that the time delays are neglected by assuming that the timescale $T_1 = \gamma^{-1}$ on which the system evolves is much larger than the photon traveling time between the two emitters.

III. TIME-CONTINUOUS MEASUREMENTS

We consider continuous measurement on the waveguide's outputs $\hat{b}_\lambda^{\text{out}}(t) = \hat{b}_\lambda^{\text{in}}(t) + \sqrt{\gamma}\hat{J}_{\lambda\pm}$, where the input vacuum

noise satisfy $[\hat{b}_\lambda^{in}(t), \hat{b}_\lambda^{in\dagger}(t')] = \delta(t - t')$. It is shown that measurements can gain information about the spin of the qubits, which render stochastic evolution of the system's state, conditioned on the measurement records [28]. The master equation (7) can be unraveled in a completely different manner, such as photon-counting detection or homodyne detection, which lead to jumpy or diffusive quantum trajectories, respectively.

For the case of photon counting, as shown in Fig. 1(c), the photodetector clicks every time, indicating it is registering a single photon emitted from the left or right outputs. With a generic detection efficiency η_λ ($\eta_\lambda \in [0, 1]$), the stochastic master equation for the conditional density matrix $\hat{\rho}_p$ is given by [29]

$$d\hat{\rho}_p = -i[\hat{\tilde{H}}_0, \hat{\rho}_p]dt - \sum_{\lambda=l,r} \gamma \mathcal{H}\left[\frac{\eta_\lambda}{2}\hat{J}_{\lambda\pm}^\dagger \hat{J}_{\lambda\pm}\right]\hat{\rho}_p dt$$

$$+ \sum_{\lambda=l,r} \gamma \mathcal{D}[\sqrt{(1-\eta_\lambda)}\hat{J}_{\lambda\pm}]\hat{\rho}_p dt$$

$$+ \sum_{\lambda=l,r} \mathcal{G}[\sqrt{\eta_\lambda}\hat{J}_{\lambda\pm}]\hat{\rho}_p dN_\lambda, \qquad (8)$$

with the symbols $\mathcal{H}[\hat{O}]\hat{\rho} = \hat{O}\hat{\rho} + \hat{\rho}\hat{O}^\dagger - \text{Tr}[\hat{O}\hat{\rho} + \hat{\rho}\hat{O}^\dagger]\hat{\rho}$ and $\mathcal{G}[\hat{O}]\hat{\rho} = \frac{\hat{O}\hat{\rho}\hat{O}^\dagger}{\text{Tr}(\hat{O}\hat{\rho}\hat{O}^\dagger)} - \hat{\rho}$. The stochastic variable $dN_\lambda(t)$ denotes the measurement results [$dN_\lambda(t) = 0$ or $dN_\lambda(t) = 1$] during an infinitesimally time interval dt. For perfect detection $\eta_\lambda = 1$, when a photon is registered [$dN_\lambda(t) = 1$], the system's state jumps to

$$|\psi_1(t + dt)\rangle \rightarrow \sum_{\lambda=l,r} \sqrt{\gamma}\hat{J}_{\lambda\pm}|\psi(t)\rangle, \qquad (9)$$

from the state $|\psi(t)\rangle$ at the time t, with the probability $\langle dN_\lambda(t)\rangle = \langle \psi(t)|\hat{J}_{\lambda\pm}^\dagger \hat{J}_{\lambda\pm}|\psi(t)\rangle dt$. When no photon is registered [$dN_\lambda(t) = 0$], the system's state collapses into

$$|\psi_0(t + dt)\rangle \rightarrow \left\{1 - \left[\sum_{\lambda=l,r} \frac{\gamma}{2}\hat{J}_{\lambda\pm}^\dagger \hat{J}_{\lambda\pm} + i\hat{\tilde{H}}_0\right]dt\right\}|\psi(t)\rangle. \qquad (10)$$

For the case of continuous homodyne detection on the waveguide's outputs, the stochastic master equation for the density operator $\hat{\rho}_c$ is [29]

$$d\hat{\rho}_c = -i[\hat{\tilde{H}}_0, \hat{\rho}_c]dt + \sum_{\lambda=l,r} \gamma \mathcal{D}[\hat{J}_{\lambda\pm}]\hat{\rho}_c dt$$

$$+ \sum_{\lambda=l,r} \sqrt{\frac{\eta_\lambda \gamma}{2}}\mathcal{H}[\hat{J}_{\lambda\pm}]\hat{\rho}_c dW_\lambda(t), \qquad (11)$$

conditioned on the detection currents

$$I_\lambda(t)dt = \sqrt{\eta_\lambda \gamma}\langle \hat{J}_{\lambda\pm} + \hat{J}_{\lambda\pm}^\dagger\rangle dt + dW_\lambda(t), \qquad (12)$$

where η_λ are homodyne detection efficiencies and $dW_\lambda(t)$ are the standard Wiener increments with mean zero and variance dt.

IV. RESULTS AND DISCUSSION

In this section, we investigate in detail the properties of the entanglement between the two qubits via photon-counting and
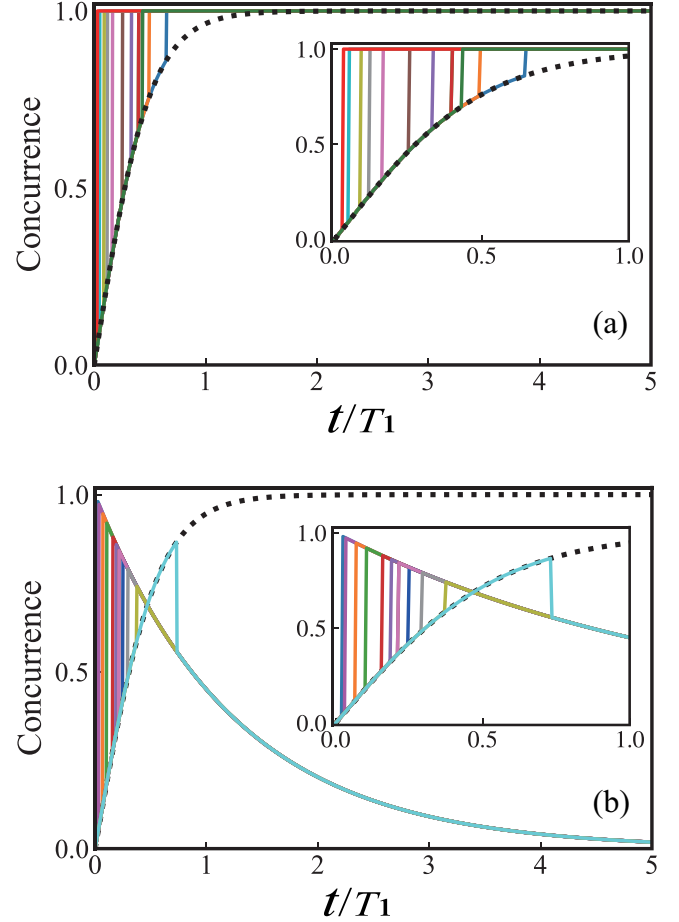

FIG. 2. The concurrence of a dozen individual jump trajectories (color solid lines) initialized from $|g_1g_2\rangle$ for (a) ideal photon detection ($\eta_l = \eta_r = 1$) and (b) inefficient photon detection ($\eta_l = \eta_r = 0.9$). The black dotted lines represent the situation where no photon is recorded during the measurement process. The parameters $kd = 2n\pi$, $T_1 = \gamma^{-1}$, and $dt = T_1/200$.

homodyne detection. The stochastic master equations (8) and (11) are numerically solved with using the PYTHON package QUTIP [44,45]. The degree of entanglement between the two emitters is measured by the concurrence [46]

$$\mathcal{C}(\hat{\rho}) = \max\{0, \lambda_1 - \lambda_2 - \lambda_3 - \lambda_4\}, \qquad (13)$$

for the density operator $\hat{\rho}$ in the basis $\{|0\rangle \equiv |g_1g_2\rangle, |1\rangle \equiv |g_1e_2\rangle, |2\rangle \equiv |e_1g_2\rangle, |3\rangle \equiv |e_1e_2\rangle\}$, where λ_i are the square roots of the eigenvalues, in decreasing order, of the non-Hermitian matrix $\hat{\rho}(\hat{\sigma}_y \otimes \hat{\sigma}_y)\hat{\rho}^*(\hat{\sigma}_y \otimes \hat{\sigma}_y)$.

A. Bell states via photon counting

In Figs. 2(a) and 2(b), we plot the time evolution of the concurrence of different jump trajectories for the initial ground state $|g_1g_2\rangle$ and the distance $kd = 2n\pi$, with the detection efficiencies $\eta_l = \eta_r = 1$ and $\eta_l = \eta_r = 0.9$, respectively. The black dotted curves represent the entanglement in the case that no photons are detected during the measurement process. It is shown that, before a photon is detected, the entanglement increases as time develops. This is clearly shown in Fig. 3(a) where the concurrence of a single trajectory is plotted.
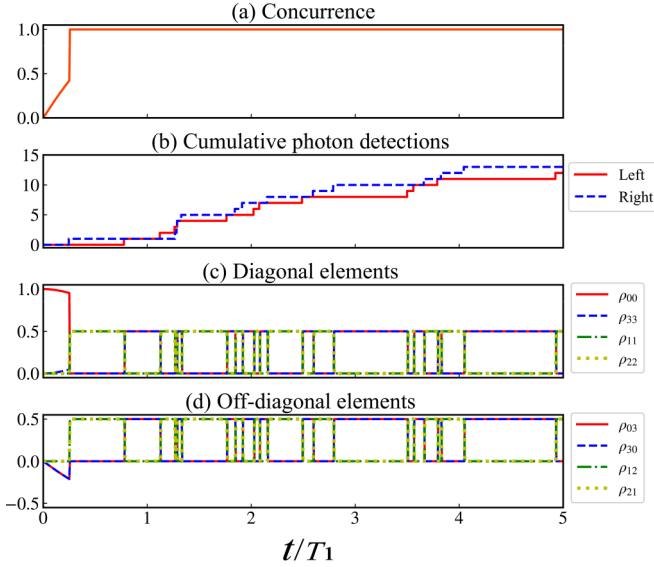
FIG. 3. (a) A single jump trajectory of concurrence, (b) cumulative photon detections at left (red solid stepped-line) and right (blue dashed stepped-line) output ports, (c) populations, and (d) coherences for perfect photon detection $\eta_l = \eta_r = 1$. The other parameters are the same as in Fig. 2.

Furthermore, after the first photon is registered, we see that the maximal concurrence $\mathcal{C} = 1$ can be always kept afterwards even in the long-time regime, which implies the two qubits are in pure Bell states. This can be understood as follows: when starting from the ground state $|g_1 g_2\rangle$, the qubits will evolve into the entangled state of the superposition between $|g_1 g_2\rangle$ and $|e_1 e_2\rangle$, as a consequence of the driving from the ground state to the excited state. Specifically, before the first photon registration (conditioning the environment being in vacuum), the system is governed by the unitary operator $\hat{U}_0(t) = \exp[(-\sum_{\lambda=l,r} \frac{1}{2} \hat{J}_{\lambda+}^\dagger \hat{J}_{\lambda+})t]$, and for the initial state $|g_1 g_2\rangle$ the system's state evolves into

$$|\psi'(t)\rangle = \frac{1 + e^{-2\gamma t}}{\sqrt{2(1 + e^{-4\gamma t})}} |g_1 g_2\rangle - \frac{1 - e^{-2\gamma t}}{\sqrt{2(1 + e^{-4\gamma t})}} |e_1 e_2\rangle, \tag{14}$$

with the concurrence

$$\mathcal{C}(t) = \frac{1 - e^{-4\gamma t}}{1 + e^{-4\gamma t}}. \tag{15}$$

We therefore see that the entanglement increases monotonically until the first photon is detected and the Bell state $|\Psi_-\rangle = (|g_1 g_2\rangle - |e_1 e_2\rangle)/\sqrt{2}$ can be achieved, conditional on the fact that no photons are detected during the time $t \gg \gamma^{-1}$.

Once a photon is registered by either detector, indicated from Eq. (14), the state $|\psi'(t)\rangle$ is then immediately projected onto the other Bell state $|\Phi_+\rangle = (|e_1 e_2\rangle + |e_1 e_2\rangle)/\sqrt{2}$ after the first jump since the information on which qubit emits the photon is erased. Moreover, this state will be maintained if no subsequent photon registration occurs because the transitions $|e_i\rangle \rightarrow |g_i\rangle$ and $|g_i\rangle \rightarrow |e_i\rangle$ simultaneously take place, according to the interaction in Eq. (6b). Until the second "click" occurs, $|\Phi_+\rangle$ jumps to a new Bell state $|\Psi_+\rangle = (|g_1 g_2\rangle + |e_1 e_2\rangle)/\sqrt{2}$ and then jumps back to state $|\Phi_+\rangle$ until some time that another photon is detected again. As a result, a cyclic
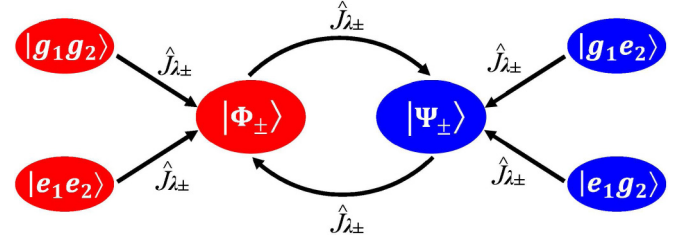

FIG. 4. A diagram of cyclic jump between Bell states $|\Phi_\pm\rangle = (|g_1 e_2\rangle \pm |e_1 g_2\rangle)/\sqrt{2}$ and $|\Psi_\pm\rangle = (|g_1 g_2\rangle \pm |e_1 e_2\rangle)/\sqrt{2}$, enabled by the jump operators $\hat{J}_{\lambda\pm} = \hat{J}_1 \pm \hat{J}_2$ on different initial states $|g_1 g_2\rangle$, $|e_1 e_2\rangle$, $|g_1 e_2\rangle$, or $|e_1 g_2\rangle$.

jump between $|\Phi_+\rangle$ and $|\Psi_+\rangle$ is formed on the condition that "clicks" take place. The concurrence thus always keeps its maximum after a transient increase. This is also exemplified in Figs. 3(b) to 3(d) where the cumulative photon-detection events, the populations, and coherence of the two qubits are, respectively, revealed for a single trajectory. It is shown that the populations of $\{\rho_{00}, \rho_{33}\}$ and $\{\rho_{11}, \rho_{22}\}$ and the corresponding coherence $\{\rho_{03}, \rho_{30}\}$ and $\{\rho_{12}, \rho_{21}\}$ take the values of 0 and 0.5 alternately after a transient growth from zero.

In fact, as illustrated in Fig. 4 where the operators $\hat{J}_{\lambda+} = \hat{J}_1 + \hat{J}_2$ and $\hat{J}_{\lambda-} = \hat{J}_1 - \hat{J}_2$, respectively, for $kd = 2n\pi$ and $kd = (2n+1)\pi$, similar state cycles between $|\Phi_\pm\rangle = (|g_1 e_2\rangle \pm |e_1 g_2\rangle)/\sqrt{2}$ and $|\Psi_\pm\rangle = (|g_1 g_2\rangle \pm |e_1 e_2\rangle)/\sqrt{2}$ can also be formed, depending on the initial states of $|g_1 g_2\rangle$, $|e_1 e_2\rangle$, $|g_1 e_2\rangle$, and $|e_1 g_2\rangle$. This is because of two possible channels for creating photons: one is the transition $|e_j\rangle \rightarrow |g_j\rangle$ via the interaction $\hat{b}_\lambda^\dagger \hat{\sigma}_j$ and the other is $|g_j\rangle \rightarrow |e_j\rangle$ through $\hat{b}_\lambda^\dagger \hat{\sigma}_j^\dagger$, according to Eq. (6b). Since the measurement is unable to distinguish from which channel the photon is created, the operator $\hat{J}_{\lambda\pm}$ can realize the following jump processes:

$$\hat{J}_{\lambda\pm} |g_1 g_2\rangle \rightarrow |e_1 g_2\rangle \pm |g_1 e_2\rangle, \tag{16a}$$

$$\hat{J}_{\lambda\pm} |g_1 e_2\rangle \rightarrow |e_1 e_2\rangle \pm |g_1 g_2\rangle, \tag{16b}$$

$$\hat{J}_{\lambda\pm} |e_1 g_2\rangle \rightarrow |g_1 g_2\rangle \pm |e_1 e_2\rangle, \tag{16c}$$

$$\hat{J}_{\lambda\pm} |e_1 e_2\rangle \rightarrow |g_1 e_2\rangle \pm |e_1 g_2\rangle. \tag{16d}$$

As discussed above, in our scheme the qubits can always be in one of the maximally entangled states due to the state cycle between $|\Phi_\pm\rangle$ and $|\Psi_\pm\rangle$. Evidently, if the interaction in Eq. (6b) only contains the terms $\hat{b}_\lambda^\dagger \hat{\sigma}_j$, as in Ref. [39], the first "click" can also herald a Bell state $|\Phi_\pm\rangle$ for the initial state $|g_1 g_2\rangle$. However, the achieved Bell state will jump back to the ground state due to spontaneous emission. It takes time to excite the qubits back to the excited states and then a subsequent "click" projects the qubits again into another Bell state. This is repeated for perfect detection efficiency. In the present scheme, because there exists the engineered terms $\hat{b}_\lambda^\dagger \hat{\sigma}_j^\dagger$, the system can always be kept in a Bell state for perfect detection.

In Fig. 2(b), the entanglement of trajectories for finite detection efficiency is plotted. We see that, under the inefficient photon detection, the concurrence of individual trajectories cannot achieve its maximal value of $\mathcal{C} = 1$ and it exhibits a clear decay after the first jump event. This is
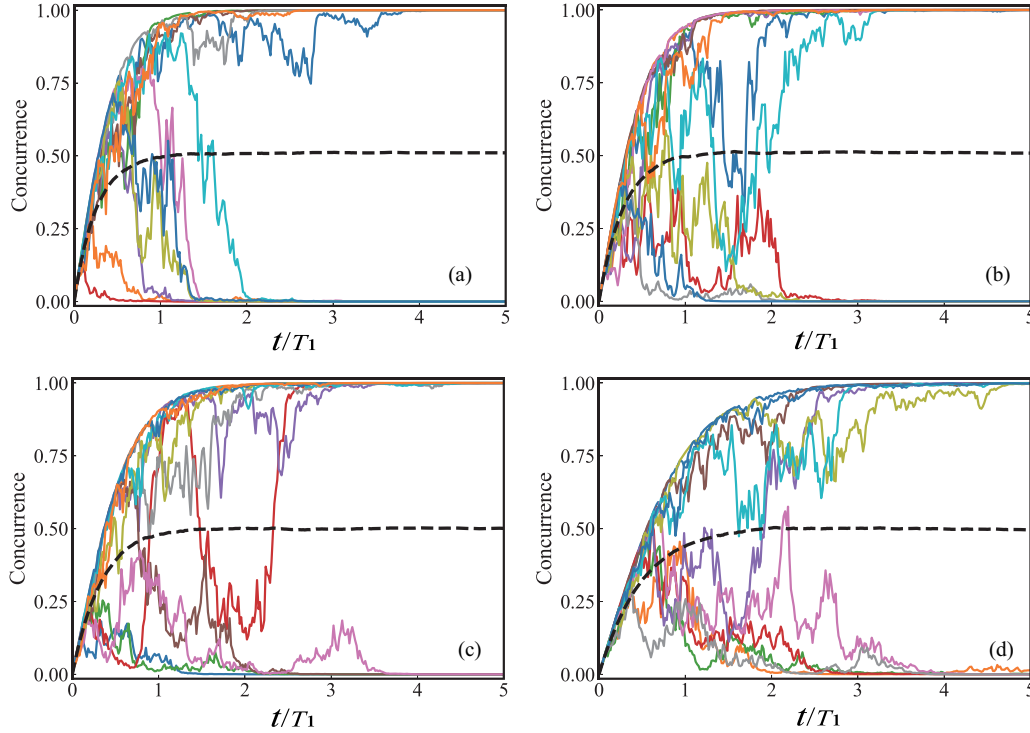
FIG. 5. The evolution of the concurrence of individual trajectories (color solid lines) and the average concurrence over an ensemble of 2000 diffusive trajectories (black dashed line) when the right outport is homodyned for initial state $|g_1 g_2\rangle$, with the detection efficiency $\eta_r = 1$ in (a), $\eta_r = 0.9$ in (b), $\eta_r = 0.75$ in (c), and $\eta_r = 0.5$ in (d). The other parameters $kd = 2n\pi$ and $T_1 = \gamma^{-1}$.

because the vacuum damping [the third terms in Eq. (8)], which models the inefficient detection, contaminates the pure Bell states. Hence, the longer the waiting time for the first "click," the less the amount of entanglement is obtained. Furthermore, the entanglement no longer increases after the first "click" and it then decays continuously whether or not photons are detected later because subsequent "clicks" do not alter the entanglement degree of the changing entangled states, but the existing vacuum damping decreases the entanglement all the time. It should be noted that recent advances in superconducting nanowire single-photon detectors (SNSPDs) have already resulted in a detection efficiency close to 100% [47].

B. Bell states via homodyne detection

In this subsection, we investigate the entanglement between the two qubits which are subject to continuous homodyne detection. We only consider one of the waveguide outputs (e.g., $\eta_l = 0$) is monitored since the same results are reached when both are homodyned. Figure 5 depicts the concurrence of some selected diffusive trajectories and the average concurrence $\overline{C}$ (dashed lines) over an ensemble of 2000 quantum trajectories for different homodyne-detection efficiencies η_r, with the initial state $|g_1 g_2\rangle$ and the distance $kd = 2n\pi$. It is clearly shown that all trajectories demonstrate short-time entanglement, some trajectories display null long-time entanglement, while the other trajectories possess steady maximal entanglement $C = 1$ independent of the detection efficiency η_r. This can be understood as follows: it can be

found from Eq. (7) the state

$$\tilde{\rho}_{ss} = \tfrac{1}{2}|\Psi_-\rangle\langle\Psi_-| + \tfrac{1}{4}(|\phi_+\rangle\langle\phi_+| + |\phi_-\rangle\langle\phi_-|), \quad (17)$$

is its possible solutions in the long-time regime, where the states $|\phi_\pm\rangle = \tfrac{1}{2}[|e_1 e_2\rangle + |g_1 g_2\rangle \pm (|g_1 e_2\rangle + |e_1 g_2\rangle)]$. Because the states $|\Psi_-\rangle$ and $|\phi_\pm\rangle$ are the eigenstates of the operator $\hat{J}_{r+}$, satisfying $\hat{J}_{r+}|\Psi_-\rangle = 0$ and $\hat{J}_{r+}|\phi_\pm\rangle = \pm|\phi_\pm\rangle$ and the unconditional equation (7) can be unraveled into a set of quantum trajectories governed by the conditional equation (11), the state $\tilde{\rho}_{ss}$ can be considered as an ensemble average of the conditioned states $|\Psi_-\rangle$ and $|\phi_\pm\rangle$ of the quantum trajectories of the homodyne detection (involved in the measurement operator $\hat{J}_{r+}$) in the steady-state regime. Since the operator $\hat{J}_{r+}$ is hermitian, its eigenstates $|\Psi_-\rangle$ and $|\phi_\pm\rangle$ satisfy the conditional equation in the steady-state regime, even the eigenvalues are nonzero for the latter and the detection is inefficient ($\eta_r < 1$). As a result, as shown in Fig. 5, the entanglement of the trajectories has the steady-state values of $C = 1$ or $C = 0$, which correspond to the states $|\Psi_-\rangle$ and $|\phi_\pm\rangle$, respectively. The steady Bell state $|\Psi_-\rangle$ can therefore be achieved with a 50% probability, which is moreover immune to the detection inefficiency. This is distinct from the case of photon counting. For finite detection efficiency, the transient states of the trajectories are still mixed and the time for approaching the steady states is prolonged as η_r decreases since less output information about the spin of the two qubits has been accessed.

From the above discussion, the average entanglement $\overline{C} = 0.5$ should be achievable in the long-time regime, as shown in Fig. 5. The explicit expression for the average concurrence in the entire time can be derived from the stochastic
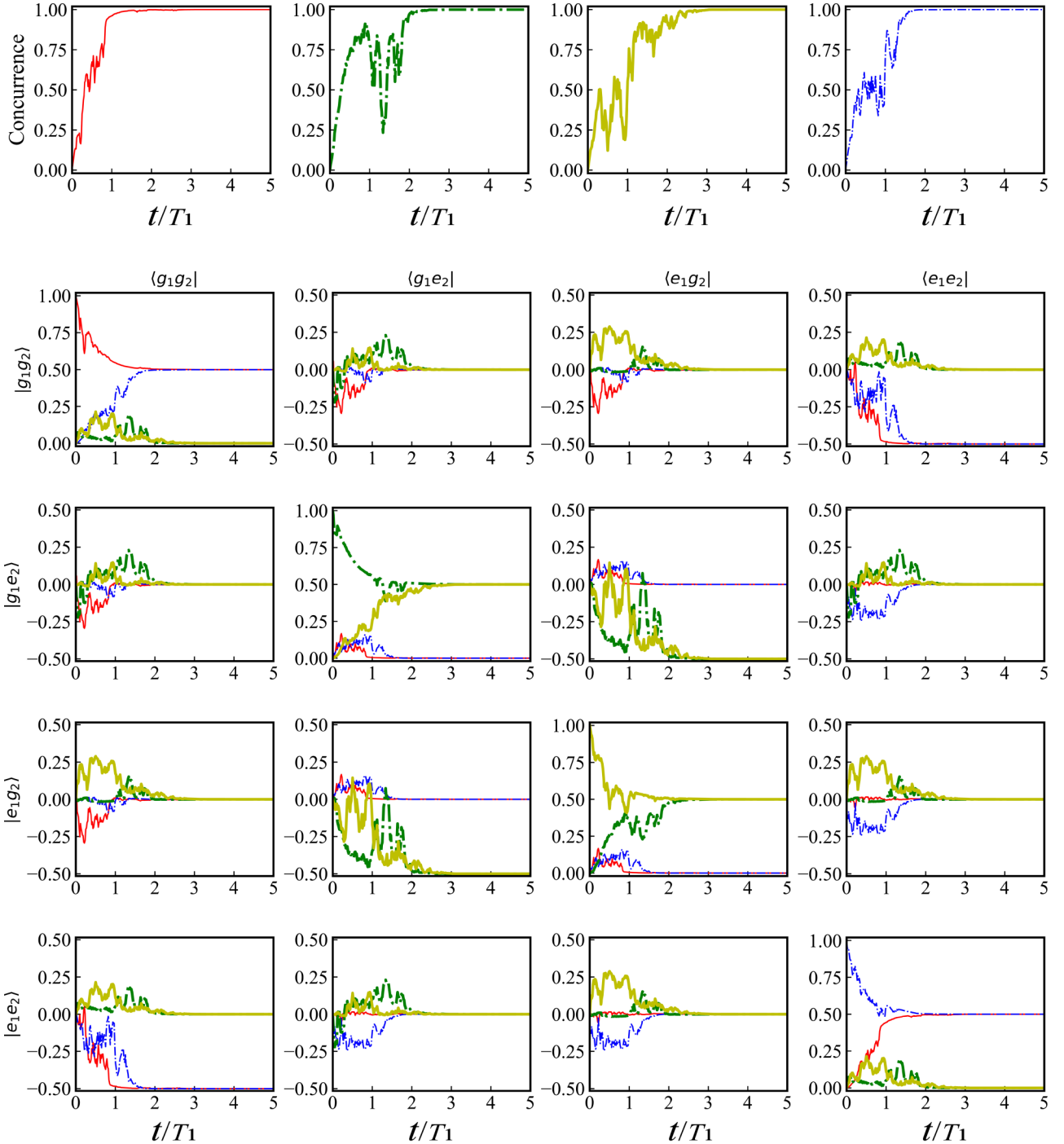
FIG. 6. (First row) Selected diffusive trajectories of the concurrence which reach the maximal values in the steady-state regime, for the initial states $|g_1 g_2\rangle$ (red thin solid line), $|g_1 e_2\rangle$ (green thick dash-dot line), $|e_1 g_2\rangle$ (yellow thick solid line), and $|e_1 e_2\rangle$ (blue thin dash-dot line). The plots in the second, third, fourth, and fifth rows are the evolution of the elements of the corresponding density matrix of each trajectory. The parameters are the same as Fig. 5.

equation (11) for $\eta_r = 1$. For a pure two-qubit state $|\widetilde{\varphi}_c\rangle = \varphi_0 |g_1 g_2\rangle + \varphi_1 |g_1 e_2\rangle + \varphi_2 |e_1 g_2\rangle + \varphi_3 |e_1 e_2\rangle$, the concurrence is $\mathcal{C} = 2|\varphi_0 \varphi_3 - \varphi_1 \varphi_2|$, and thus the evolution of the concurrence $\mathcal{C}$ is derived as

$$dC(\widetilde{\varphi}_c) = |-3\gamma C(\widetilde{\varphi}_c)dt + 3\gamma(\varphi_1^2 + \varphi_2^2 - \varphi_0^2 - \varphi_3^2)dt - 2\sqrt{\gamma}C(\widetilde{\varphi}_c)\langle \hat{J}_{r+}\rangle dW_r|, \quad (18)$$

from which the ensemble average of the concurrence can be calculated as

$$\overline{C}(\widetilde{\varphi}_c) = \frac{1}{2} - \frac{1}{5}e^{-3\gamma t} - \frac{3}{10}e^{-8\gamma t}, \quad (19)$$

for the initial state $|g_1 g_2\rangle$, which coincides with the numerical result.

In Fig. 6, the entanglement of trajectories for different initial states are plotted. We specifically choose four

individual trajectories whose concurrence $\mathcal{C} = 1$ in the long-time limit, for the initial states $|g_1 g_2\rangle$, $|g_1 e_2\rangle$, $|e_1 g_2\rangle$, and $|e_1 e_2\rangle$, respectively. In addition, the corresponding populations and coherences are also plotted. Note that, similar to Fig. 5, the entanglement of the trajectories for these initial states also becomes $\mathcal{C} = 1$ or $\mathcal{C} = 0$ in the steady-state regime. It is shown that the individual trajectory initialized at $|g_1 g_2\rangle$ (red thin solid line) or $|e_1 e_2\rangle$ (blue thin dash-dot line) eventually evolves into the Bell state $|\Psi_-\rangle$, while the trajectory started from $|g_1 e_2\rangle$ (green thick dash-dot line) or $|e_1 g_2\rangle$ (yellow thick solid line) asymptotically approaches another Bell state $|\Phi_-\rangle$. This is different from the cyclic jumps in the previous case of photon counting. It should be pointed out that if the distance of the two qubits satisfies $kd = (2n + 1)\pi$, the steady Bell states $|\Psi_+\rangle$ or $|\Phi_+\rangle$ of the trajectories can be resulted, respectively, for the initial states $|g_1 g_2\rangle$ ($|e_1 e_2\rangle$) or $|e_1 g_2\rangle$ ($|g_1 e_2\rangle$). Therefore, from the discussion, continuous homodyne measurement can also allow us to probabilistically generate long-time Bell states via making a postselection on the diffusive trajectories with the long-time concurrence $\mathcal{C} = 1$.

V. DISCUSSION AND CONCLUSION

Before concluding, let us briefly introduce the experimental feasibility of our scheme. In our experimental consideration, a nanoscale photonic crystal waveguide, two identical alkali-metal atoms, high efficiency detectors (e.g., SNSPDs), and appropriate laser sources are preferred. The rubidium 87 D_2 transition (on the $5S_{1/2} - 5P_{3/2}$ at 780 nm) hyperfine structure [48] can be considered as a possible candidate to form a Λ-level scheme, for example, $|g\rangle = |5S_{1/2}F = 1\rangle$, $|e\rangle = |5S_{1/2}F = 2\rangle$, and $|i\rangle = |5P_{3/2}F' = 1\rangle$. The relaxation rate Γ_{eg} of coherence between states $|e\rangle$ and $|g\rangle$ is so small that it can be negligible in our consideration. As designed in Fig. 1(a), position two spatially separated singly

trapped atoms in the evanescent field located outside the photonic crystal waveguide. In this region, the atoms are driven by two controllable laser fields at Rabi frequencies $\Omega_{a,b}$, and simultaneously couple to the waveguide-bath via two off-resonant Raman transitions with single-photon Rabi frequency g. The coupling strength can be tuned in the range of several GHz by precisely controlling the atom-surface distances [49,50]. The parameters can be set as the experimentally feasible conditions as follows: $g \simeq 10$ MHz, $|\Omega_{a,b}| \simeq 10g$ and $|\Delta_{a,b}| \simeq 100g$, so that $\gamma \simeq 2\pi \times 4$ MHz and $T_1 \simeq 0.25\,\mu$s.

In conclusion, we show in this paper how to prepare long-term sustainable Bell states of two distant qubits by using time-continuous photon counting or homodyne detection. We consider two identical Λ emitters which are coupled to a one-dimensional waveguide via off-resonant Raman scattering. It is shown that, in both of these detection schemes, Bell states can be realized in the long-time regime. For the case of photon counting, a cyclic jump among Bell states can be formed and the alternate appearance of different Bell states is heralded on the subsequent photon-detection events in the long-time regime. While for the case of homodyne detection, it is found that different Bell states can be achieved in the regime of steady states with a probability of 50%, independent of the detection efficiency. Our scheme is advantageous over previous ones in which transient or intermittent Bell states of qubits can only be generated, and it may find applications in, e.g., quantum communication networks.

ACKNOWLEDGMENTS

[1] M. A. Nielsen and I. L. Chuang, *Quantum Computation and Quantum Information* (Cambridge University Press, Cambridge, England, 2002).

[2] C. H. Bennett, G. Brassard, C. Crépeau, R. Jozsa, A. Peres, and W. K. Wootters, Phys. Rev. Lett. **70**, 1895 (1993).

[3] D. Shwa, R. D. Cohen, A. Retzker, and N. Katz, Phys. Rev. A **88**, 063844 (2013).

[4] L. Quiroga and N. F. Johnson, Phys. Rev. Lett. **83**, 2270 (1999).

[5] Z. Leghtas, U. Vool, S. Shankar, M. Hatridge, S. M. Girvin, M. H. Devoret, and M. Mirrahimi, Phys. Rev. A **88**, 023849 (2013).

[6] H. Y. Yuan, Peng Yan, Shasha Zheng, Q. Y. He, Ke Xia, and Man-Hong Yung, Phys. Rev. Lett. **124**, 053602 (2020).

[7] J. I. Cirac, P. Zoller, H. J. Kimble, and H. Mabuchi, Phys. Rev. Lett. **78**, 3221 (1997).

[8] H. J. Kimble, Nature (London) **453**, 1023 (2008).

[9] P. Bermel, A. Rodriguez, S. G. Johnson, J. D. Joannopoulos, and M. Soljačíc, Phys. Rev. A **74**, 043818 (2006).

[10] H. Zheng, D. J. Gauthier, and H. U. Baranger, Phys. Rev. Lett. **111**, 090502 (2013).

[11] P. Longo, P. Schmitteckert, and K. Busch, Phys. Rev. Lett. **104**, 023602 (2010).

[12] D. Witthaut and A. S. Sørensen, New J. Phys. **12**, 043052 (2010).

[13] H. Zheng, D. J. Gauthier, and H. U. Baranger, Phys. Rev. A **82**, 063816 (2010).

[14] E. Rephaeli, S. E. Kocabas, and S. Fan, Phys. Rev. A **84**, 063832 (2011).

[15] D. Roy, Phys. Rev. Lett. **106**, 053601 (2011).

[16] P. Kolchin, R. F. Oulton, and X. Zhang, Phys. Rev. Lett. **106**, 113601 (2011).

[17] E. Rephaeli and S. Fan, Phys. Rev. Lett. **108**, 143602 (2012).

[18] A. Akimov, A. Mukherjee, C. Yu, D. Chang, A. Zibrov, P. Hemmer, H. Park, and M. Lukin, Nature (London) **450**, 402 (2007).

[19] D. E. Chang, J. I. Cirac, and H. J. Kimble, Phys. Rev. Lett. **110**, 113606 (2013).

[20] A. Goban, C.-L. Hung, S.-P. Yu, J. Hood, J. Muniz, J. Lee, M. Martin, A. McClung, K. Choi, D. Chang *et al.*, Nat. Commun. **5**, 3808 (2014).

[21] C. Rigetti, J. M. Gambetta, S. Poletto, B. L. T. Plourde, J. M. Chow, A. Čorcoles, J. A. Smolin, S. T. Merkel, J. Rozen, G. A. Keefe, M. B. Rothwell, M. B. Ketchen, and M. Steffen, Phys. Rev. B **86**, 100506(R) (2012).

[22] J.-B. Béguin, E. M. Bookjans, S. L. Christensen, H. L. Sørensen, J. H. Müller, E. S. Polzik, and J. Appel, Phys. Rev. Lett. **113**, 263603 (2014).

[23] C. Gonzalez-Ballestero, E. Moreno, and F. J. Garcia-Vidal, Phys. Rev. A **89**, 042328 (2014).

[24] C. Gonzalez-Ballestero, A. Gonzalez-Tudela, F. J. Garcia-Vidal, and E. Moreno, Phys. Rev. B **92**, 155304 (2015).

[25] D. Martín-Cano, A. González-Tudela, L. Martín-Moreno, F. J. Garcia-Vidal, C. Tejedor, and E. Moreno, Phys. Rev. B **84**, 235306 (2011).

[26] A. González-Tudela, D. Martín-Cano, E. Moreno, L. Martín-Moreno, C. Tejedor, and F. J. Garcia-Vidal, Phys. Rev. Lett. **106**, 020501 (2011).

[27] L. Trifunovic, F. L. Pedrocchi, and D. Loss, Phys. Rev. X **3**, 041023 (2013).

[28] H. Carmichael, *An Open System Approach to Quantum Optics* (Springer, Berlin, 1993).

[29] H. M. Wiseman and G. J. Milburn, *Quantum Measurement and Control* (Cambridge University Press, Cambridge, England, 2009).

[30] J. Zhang, Y.-X. Liu, R.-B. Wu, K. Jacobs, and F. Nori, Phys. Rep. **679**, 1 (2017).

[31] S. Vogelsberger and D. Spehner, Phys. Rev. A **82**, 052327 (2010).

[32] C. Viviescas, I. Guevara, A. R. R. Carvalho, M. Busse, and A. Buchleitner, Phys. Rev. Lett. **105**, 210502 (2010).

[33] R. Ruskov and A. N. Korotkov, Phys. Rev. B **67**, 241305(R) (2003).

[34] N. Roch, M. E. Schwartz, F. Motzoi, C. Macklin, R. Vijay, A. W. Eddins, A. N. Korotkov, K. B. Whaley, M. Sarovar, and I. Siddiqi, Phys. Rev. Lett. **112**, 170501 (2014).

[35] F. Motzoi, K. B. Whaley, and M. Sarovar, Phys. Rev. A **92**, 032308 (2015).

[36] P. Lewalle, C. Elouard, S. K. Manikandan, X.-F. Qian, J. H. Eberly, and A. N. Jordan, arXiv:1910.01204.

[37] O. Černotík and K. Hammerer, Phys. Rev. A **94**, 012340 (2016).

[38] A. Chantasri, M. E. Kimchi-Schwartz, N. Roch, I. Siddiqi, and A. N. Jordan, Phys. Rev. X **6**, 041052 (2016).

[39] X. H. H. Zhang and H. U. Baranger, Phys. Rev. Lett. **122**, 140502 (2019).

[40] L. Zhou, L. P. Yang, Yong Li, and C. P. Sun, Phys. Rev. Lett. **111**, 103604 (2013).

[41] T. Werlang, R. Guzmán, F. O. Prado, and C. J. Villas-Bôas, Phys. Rev. A **78**, 033820 (2008).

[42] Z. Ficek and R. Tanaś, Phys. Rep. **372**, 369 (2002).

[43] H. Pichler, T. Ramos, A. J. Daley, and P. Zoller, Phys. Rev. A **91**, 042116 (2015).

[44] J. R. Johansson, P. D. Nation, and F. Nori, Comput. Phys. Commun. **183**, 1760 (2012).

[45] J. R. Johansson, P. D. Nation, and F. Nori, Comput. Phys. Commun. **184**, 1234 (2013).

[46] W. K. Wootters, Phys. Rev. Lett. **80**, 2245 (1998).

[47] D. V. Reddy, R. R. Nerem, S. W. Nam, R. P. Mirin, and V. B. Verma, Optica **7**, 1649 (2020).

[48] D. A. Steck, http://steck.us/alkalidata/rubidium87numbers.pdf.

[49] J. D. Thompson, T. G. Tiecke, N. P. de Leon, J. Feist, A. V. Akimov, M. Gullans, A. S. Zibrov, V. Vuletić, and M. D. Lukin, Science **340**, 6137 (2013).

[50] C.-L. Hung, S. M. Meenehan, D. E. Chang, O. Painter, and H. J. Kimble, New J. Phys. **15**, 083026 (2013).